

2D Nanomaterial, Ti₃C₂ MXene Based Sensor to Guide Lung Cancer Therapy and Management †

Danling Wang ^{1,2,3,*}, Mahek Sadiq ², Lizhi Pang ⁴, Michael Johnson ³ and Sathish Venkatachalem ⁴

¹ Department of Electrical and Computer Engineering, North Dakota State University, Fargo, ND 58102, USA

² Biomedical Engineering Program, North Dakota State University, Fargo, ND 58102, USA;

³ Materials and Nanotechnology Program, North Dakota State University, Fargo, ND 58108, USA;

⁴ Department of Pharmaceutical Science, North Dakota State University, Fargo, ND 58108, USA;

* Correspondence: danling.wang@ndsu.edu; Tel.: +86-10-701-231-8396

† Presented at the 1st International Electronic Conference on Biosensors, 2–17 November 2020; Available online: <https://iecb2020.sciforum.net/>.

Received: date; Accepted: date; Published: date

Abstract: Major advances in cancer control can be greatly aided by early diagnosis and effective treatment in its pre-invasive state. Lung cancer (small cell and non-small cell) is a leading cause of cancer-related death among both men and women around the world. A lot of research attention has been attracted to diagnose and treat lung cancer. Common method of lung cancer treatment is based on COX-2 (Cyclooxygenase-2) inhibitors. This is because COX-2 is commonly over expressed in lung cancer and also the abundance of its enzymatic product Prostaglandin E₂ (PGE₂). Instead of using traditional COX-2 inhibitors to treat lung cancer, here, we report a new anti-cancer strategy recently developed for lung cancer treatment. It adopts more abundant omega-6 (ω -6) fatty acids such as dihomo- γ -linolenic acid (DGLA) in the daily diet and the commonly high levels of COX expressed in lung cancer to promote the formation of 8-hydroxyoctanoic acid (8-HOA) through a new delta-5-desaturase (D5Di) inhibitor. The D5Di will not only limit the metabolic product, PGE₂ but also promote the COX-2 catalyzed DGLA peroxidation to form 8-HOA, a novel anti-cancer free radical byproduct. Therefore, the measurement of the PGE₂ and 8-HOA levels in cancer cells can be an effective method to treat lung cancer by providing in-time guidance. A novel sensor based on a newly developed functionalized nanomaterial, 2-dimensional nanosheets, Ti₃C₂ MXene, has proved to sensitively, selectively, precisely and effectively detect PGE₂ and 8-HOA in A549 lung cancer cells. Due to multilayered structure and extreme large surface area, metallic conductivity and easy and versatile in surface modification, Ti₃C₂ Mxene based sensor will be able to selectively adsorb different molecules through physical adsorption or electrostatic attraction, and lead to a measurable change in the conductivity of the material with high signal to noise ratio and excellent sensitivity.

Keywords: 2D Ti₃C₂ Mxene; PGE₂; 8-HOA; lung cancer

1. Introduction

The most common cancers occur in lung, breast, pancreas, colon, skin and stomach [1]. Lung cancer is the second most common cancer in men and women and the first leading cause of cancer deaths in the United States. The two major types of lung cancer are: small cell lung cancer (SCLC, ~15%) [2] and non-small cell lung cancer (NSCLC, ~85%) [3]. The survival rate of both types of lung cancer is very low [4]. According to the American Cancer Society, lung cancer and asbestos related lung cancer [5] alone is responsible for 142,670 estimated deaths in 2019, making it the number one killer and three times deadlier than breast cancer [6]. This is because most patients (~75%) have been diagnosed at a late stage of the disease (stage III or IV) [7]. To increase the survival rate, major

advances in lung cancer control or prevention will be greatly aided by early detection and effective anti-cancer therapy. In recent years, a variety of therapeutic and adjuvant methods and nutritional approaches have been developed for lung cancer treatment such as chemotherapy, targeted therapy [8,9], cyclooxygenase (COX)-2 inhibition [10], and omega-3 fatty acid dietary manipulation [11,12].

Besides these methods, many physical ‘visualization/detection’ methods [13] are available for tumor detection and cancer diagnosis [14]. Some of them are, Positron Emission Tomography (PET), Magnetic resonance imaging (MRI), Computerized Tomography (CT), Ultrasonography, Endoscopy and Gas Chromatography method. However, these methods have some major issues for applications in cancer diagnosis. For example, MRI is very expensive and time consuming. Sometimes it even cannot distinguish between malignant and benign cancer [15]. In case of PET, radioactive material is used which is combined with glucose and injected into the patient. This might be a health concern for diabetic patients [16]. High dose radiations involved in CT scanning can even increase the risk of cancer [17]. Ultrasound, however, cannot provide accurate diagnosis and frequently has trouble to determine whether a mass is malignant or not [18]. Endoscopy is relatively safer but still has complications like perforation, infection, bleeding, and pancreatitis [19]. The fundamental limitation of gas chromatography is that the substance must be volatile. It means that a finite portion of the substance needs to be distributed into the gaseous state [20]. It is problematic to use Gas Chromatography Mass Spectroscopy (GC-MS) in cancer detection because its sampling procedure is very complicated and the results are difficult to interpret. This technique is very expensive and must be operated by a very skilled personnel [21]. Therefore, an effective and accurate technique to detect tumor and diagnose cancer is urgently needed.

In particular, studies have confirmed that cyclooxygenase (COX), typically the inducible form COX-2, is commonly over expressed in lung cancer and the abundance of its enzymatic product prostaglandin E₂ (PGE₂) plays an important role in influencing the cancer development. Since PGE₂ is a deleterious metabolite formed from COX-2-catalyzed peroxidation of an upstream omega-6 (ω -6) fatty acid called arachidonic acid (AA), PGE₂ promotes tumor growth and metastasis [22]. So, it can be taken as an indicator of local COX activity to regulate or control lung cancer. A lot of efforts on treating lung cancer have been focused on the development of COX-2 inhibitors because they can be used to suppress prostaglandin E₂ (PGE₂) formation from COX-2-catalyzed ω -6 arachidonic acid peroxidation [23]. However, most COX-2 inhibitors can severely injure the gastrointestinal tract, increase the risk of cardiovascular disease, and provide limited clinical responses [22,23]. To seek a safer and more efficient method to treat cancers, a new anti-cancer strategy [24], as shown in Figure 1., has been recently developed which is a very different approach than the classic COX-2 inhibitors [24–26]. In detail, this is a strategy which adopts more abundant ω -6s such as dihomo- γ -linolenic acid (DGLA) in the daily diet and the commonly high level of COX expressed in most cancers to promote the formation of 8-hydroxyoctanoic acid (8-HOA) through using a newly developed inhibitor, delta-5-desaturase (D5Di) inhibitor. This is because the D5D is an enzyme that converts an upstream DGLA in diet to AA. The high expression of COX-2 will promote the conversion of AA to PGE₂. While the D5Di will 1) knock down the conversion of DGLA to AA and limit the metabolic product, PGE₂; 2) promote the COX-2 catalyzed DGLA peroxidation to form 8-HOA, a novel anti-cancer free radical by product. This strategy has proven to produce more effective and safer therapeutic outcomes in cancer treatment and validate in the colon and pancreatic cancers [27]. Therefore, detection of the PGE₂ and 8-HOA in lung cancer should be an effective method to evaluate the efficiency of the cancer treatment. Also, the relative ratio of PGE₂ and 8-HOA concentrations can become a useful adjuvant method to help diagnose cancers at an early stage. Therefore, it is very critical to develop a technique or device, which can track PGE₂ and 8-HOA concentrations in cancer and provide in-time guidance and feedback for cancer treatment and prevention. However, due to the extreme low concentrations of PGE₂ and 8-HOA in cancer cells ~ ng/mL or μ M, the detection of these components is quite challenging. Traditional method to measure low concentration of compounds such as, PGE₂ and 8-HOA is using gas chromatography-mass spectrometry (GC-MS) or liquid chromatography-mass spectrometry (LC-MS). These techniques, as described above, are accurate and sensitive but heavy (not portable), expensive (skilled personnel to operate), and time-consuming. Recent advances in

nanofabrication technology have made it possible to be widely used in electronics, sensing, biomaterials for variable areas including disease diagnosis and control in medicine, drug delivery, and food industry [28–31]. Due to the increased surface areas and the feasibility of controllable size and surface properties, nanomaterials such as nanofibers, nanowires, nanoparticles provide great opportunities for the development of advanced sensing systems and portable device/instrumentation with improved sensitivity, and selectivity [32–38]. In particular, the use of structure-directing synthetic approaches in nanomaterial synthesis allows the preparation of particularly promising nanomaterials by tailoring nanomaterial crystalline phase, surface states, morphology, and facets for specific sensing application. With the development of two-dimensional (2D) nanomaterials such as graphene, these type of materials have gained tremendous attention because of their astonishing electrical and optical properties featured with “all-surface” nature [39–43]. Such all-surface nature can offer great opportunities to tailor material properties through surface treatment for targetable detection. In 2011, the birth of MXenes introduced a new family into the two-dimensional (2D) materials and further proves to be promising in the flexible sensory application due to its controllable preparation method and fascinating properties. In essence, MXenes consists of transition metals (including Ti, V, Nb, Mo, etc.) and carbon or nitrogen, sharing a general formula of $M_{n+1}X_n$ ($n = 1-9$). As a new star of 2D materials, MXenes have the metallic conductivity and hydrophilic nature due to their uncommon surface terminations. The unique accordion-like morphology (Figure 2), excellent conductivity, and rich but tailorable surface functional groups endow MXenes with attractive electronic, mechanical, physical and chemical properties for applications in energy storage [44], environmental science [45], and sensors [46]. In this paper, we report a new sensor based on a newly developed 2-dimensional nanomaterial, Ti_3C_2 MXene. The preliminary data indicate that this device can sensitively detect PGE_2 and 8-HOA levels in healthy and cancerous lung cells (BEAS2B and A549 respectively) in order to validate the effectivity of this new strategy in lung cancer treatment as well as in-time guidance during the therapy.

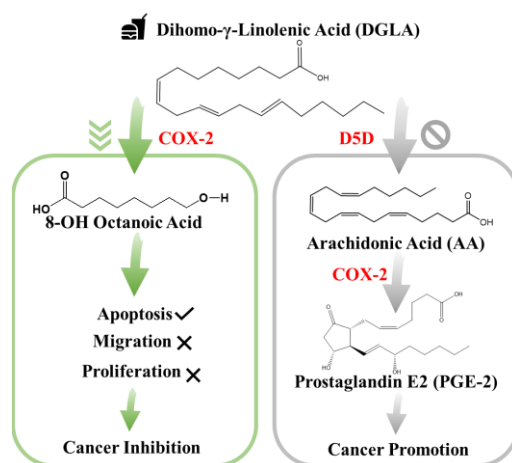


Figure 1. New anticancer strategy: target but not inhibit COX-2 in cancer.

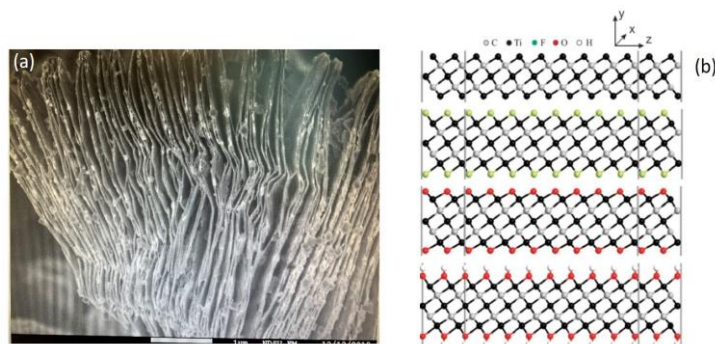


Figure 2. Newly synthesized 2D multi-layered Ti_3C_2 MXene nanosheets (a) Scanning Electron Microscope (SEM) image; (b) Pristine and surface-terminated Ti_3C_2 MXene with different functional groups.

2. Materials and Methods

2.1. Sensing Material Synthesis and Cell Lines Preparation

2.1.1. Ti_3C_2 Nanomaterial Based Sensor Preparation

The sensor that we used is based on a new 2-D nanomaterial, Ti_3C_2 MXene. This nanomaterial was prepared using a method developed in our group, named as the 'hot etching method' [47,48]. In details, the synthesis of Ti_3C_2 MXene followed the steps: (1) Preparing Ti_3AlC_2 MAX phase. It was obtained through ball milling TiC, Ti, Al powders in the molar ratio 2:1:1.2 for 5 h. Under argon flow, the resulting powder was then pressed into a pellet and sintered at 1350 °C for 4 h. The collected pellet after being milled back into powder was sieved through a 160-mesh sieve; (2) Etching Al from MAX phase to form MXene phase. The as-prepared MAX powder was collected at an elevated temperature for etching through 'hot-etch method'. HF acid in 25 mL Teflon line autoclave at a temperature of 150 °C was used in a Thermolyne furnace for 5 h to etch 0.5 g of MAX phase. 5 %wt of HF were used to remove Al from MAX phase. Materials after being sonicated for one hour using a sonicating bath were collected through centrifuge; All the materials were dried overnight in a drying oven at 65 °C (3) Synthesizing MXene powders for the sensing film. Finally, the synthesized nanomaterial was drop-casted on the gold electrode patterned glass substrate to form a thin film. The morphology of the synthesized 2D multilayered nanomaterial is shown in Figure 2a as the scanning electron microscope (SEM) image, which clearly exhibits multi-layered nanosheets and accordion-like morphology. Figure 2b reveals the as-synthesized Ti_3C_2 material's special surface terminations, which can lead to unique surface and material properties of Ti_3C_2 .

2.1.2. Cancer Cell Lines and Materials

A549 (ATCC® CCL-185™), and BEAS-2B (ATCC® CRL-9609™) were purchased from American Type Culture Collection (ATCC, VA, USA). Iminodibenzyl (CAS Number: 494-19-9) and 8-hydroxyoctanoic acid (8-HOA) were obtained from Sigma-Aldrich (MO, USA). PGE₂ and DGLA (for in vitro study), DGLA ethyl ester (for in vivo study), were acquired from Cayman Chemical (MI, USA).

2.1.3. Preparation of Cell Samples

About 3×10^5 A549 or BEAS-2B cells were trypsinized and seeded into each well of the 6-well plates. Then the cells were randomly assigned into different groups for the administration of DGLA (100 μM), iminodibenzyl (10 μM), or their combination accordingly. After 48 h, the cell culture medium was collected. Cells were washed with PBS and collected by centrifugation after trypsinization. 1 mL cell culture medium with collected cells was homogenate and ready for testing. Three different groups of control samples were prepared as the same preparation procedures, including (a) blank group in 1 mL cell homogenate without any treatment; (b) 8-HOA group in 1 mL cell homogenate containing 0.6 ug/mL exogenous 8-HOA; (c) PGE₂ group in 1 mL cell homogenate containing 6 ug/mL exogenous PGE₂.

2.1.4. Xenografted Lung Tumor Model on Nude Mice

Six-week-old nude mice (nu/nu) mice were purchased from The Jackson Laboratory. The mice were housed in a pathogen-free IVC System with water and food ad libitum. All the animal experiments in this study were approved by the Institutional Animal Care and Use Committees at North Dakota State University. About 2×10^6 A549 cells were injected into the hind flank of the nude mouse to induce tumors as we previously described [26]. The mice were randomly assigned to the

following treatments: Control (treated with the same volume of the vehicle), DGLA (5 mg/mouse, oral gavage, every day), iminodibenzyl (15 mg/kg, intraperitoneal injection, every day), and DGLA + iminodibenzyl. The treatment was started at two weeks of injection of A549 cells in nude mice. All the administrations lasted for four weeks. At end of the treatment, mice were sacrificed and tumors were isolated. Tumor tissues were crushed and homogenized by using a mortar in liquid nitrogen. The blood was centrifuged for 10 min at 2000 rpm for separating serum. The supernatant of tumor tissues and serum was collected for analysis.

2.2. Methodology

To verify the roles of 8-HOA and PGE₂ in cancer development and treatment, the experiments have been designed to do testing in healthy lung cells and A549 lung cancer cells.

-Normal cells

10⁶ BEAS2B non-tumorigenic epithelial cell lines were collected for application to do testing of the effect of 8-HOA and PGE₂ in normal lung cells. 8-HOA, PGE₂ and BSA (Bovine Serum Albumin) were applied to the samples right before measuring the resistance change. Once the samples were applied onto the Ti₃C₂ MXene based sensors, resistances were measured immediately and repeated at regular time intervals. The experiment is listed in the Table 1 and the resistance change of the MXene slides for each of the samples is measured and shown in Figure 3. The resistance increases dramatically when BEAS2B with PGE₂ is added but BEAS2B alone and BEAS2B with 8-HOA does not show obvious change of resistance.

Table 1. Table showing the composition of each sample for BEAS2B.

Sample	Cell	8-HOA	PGE ₂	BSA
1	10 ⁶ BEAS2B	none	none	None
2	10 ⁶ BEAS2B	0.6 ug/mL	none	None
3	10 ⁶ BEAS2B	none	6 ug/mL	None
4	None	none	none	1 mg/mL

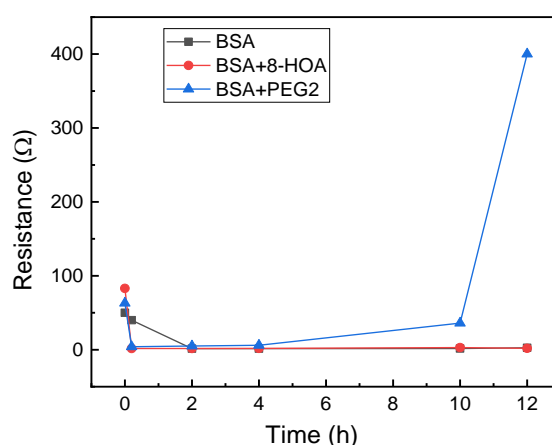


Figure 3. Resistance change measured using Ti₃C₂MXene based sensors for BEAS2B cells.

-A549 lung cancer cells

A549 lung cancer epithelial cell lines were collected after being cultured. Similar to the BEAS-2B cell lines, 8-HOA and PGE₂ samples were applied to the A549 cell lines just before conducting the experiment. The complete design of the experiments to verify the relative concentration of generated 8-HOA and PGE₂ with and without using the new cancer treatment are listed in the Table 2.

Table 2. The composition of each sample for A549 cells treated by 8-HOA, PGE₂, DGLA, D5Di and DGLA + D5Di.

Sample	Cell	DGLA	D5Di	8-HOA	PGE ₂	Estimated 8-HOA/PGE ₂ Level
1	10 ⁶ A549	none	none	none	none	Low 8-HOA; low PGE ₂
2	10 ⁶ A549	none	none	0.6 ug/mL	none	High 8-HOA; low PGE ₂
3	10 ⁶ A549	none	none	none	6 ug/mL	Low 8-HOA; high PGE ₂
4	10 ⁶ A549	100 uM	none	none	none	Low 8-HOA; high PGE ₂
5	10 ⁶ A549	none	10 uM	none	none	Low 8-HOA; low PGE ₂
6	10 ⁶ A549	100 uM	10 uM	none	none	High 8-HOA; low PGE ₂

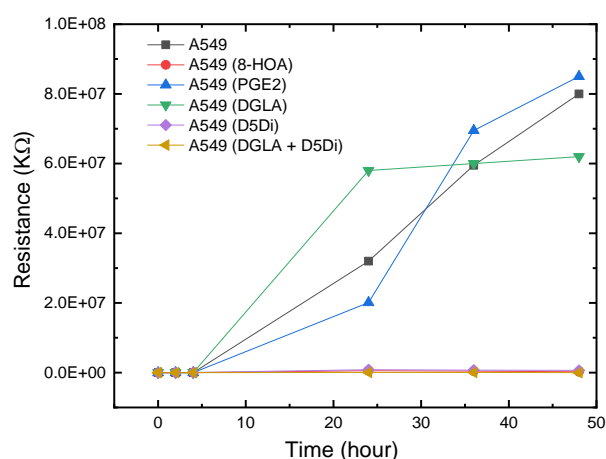


Figure 4. Resistance change measured using Ti₃C₂MXene based sensors for A549 cancer cells with and without using the new anti-cancer treatment.

The sensing tests of these samples have been shown in Figure 4. The resistances of A549 cancer cells, A549 cells treated by DGLA, and PGE₂ are much higher than the cancer cells treated by adding 8-HOA, applying D5Di, or using the new anti-cancer treatment DGLA + D5Di.

3. Results and Discussion

3.1. Observation from the Non-Tumorigenic Sample Graph

In a healthy subject, both the concentration of PGE₂ and 8-HOA should be low. The sensing test is conducted on the normal lung cell, BEAS2B without extra treatment and BEAS2B by treating with extra PGE₂ or 8-HOA. Significant resistance increase is observed in BEAS2B by adding 10 μM PGE₂ while the untreated normal cells and cells treated by 8-HOA do not show obvious resistance change. This result indicates a unique role of PGE₂ in cells through the change of electrical property of cells. Considering the elevated concentration of PGE₂ can indicate a cancer development, such a sensitive response to PGE₂ using Ti₃C₂MXene based sensor can be potentially used to diagnose cancer even at a very early stage.

3.2. Observation from the CARCINOGENIC Samples (1st Trial)

As we have discussed in this paper previously, D5D inhibitor (D5Di) is used for preventing the conversion of DGLA to AA and ultimately limiting the formation of PGE₂. According to the main mechanism of the new anti-cancer strategy, D5Di along with DGLA can effectively limit the formation of PGE₂ but promote the formation of 8-HOA. The sensing test using the newly developed Ti₃C₂MXene based sensor, as shown in Figure 4, exhibits an interesting trend of resistance change. Similar to showing high resistance for A549, A549 with adding 10uM PGE₂, and A549 treated by

DGLA both show high resistance as well. The results indicate a higher concentration of PGE₂ generated in A549 cells just by using DGLA, which confirms that omega-6 (DGLA) are pro-inflammatory and promote the formation of PGE₂. However, the new anti-cancer treatment using DGLA and D5Di to treat A549 cells shows the similar resistance level as that of A549 cells with 8-HOA. This result provides promising information: the Ti₃C₂ MXene based sensor can be used to monitor or validate the anti-cancer effect of the new strategy: DGLA + D5Di, which should be an effective anti cancer effect due to the generation of 8-HOA. This result is consistent with the results using GC-MS to confirm the new anti-cancer effect, as shown in Figure 5 [49].

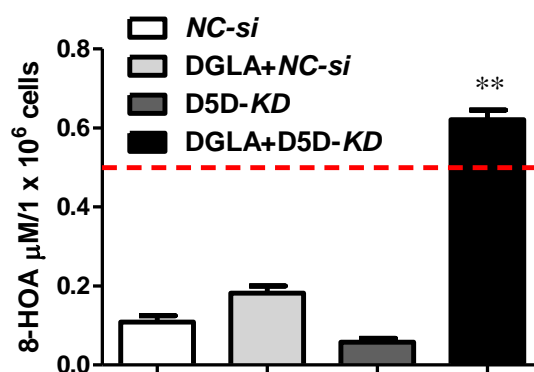


Figure 5. Effect of DGLA and D5D siRNA on 8-HOA formation.

4. Conclusions and Discussion

The preliminary results lead to an important conclusion: Ti₃C₂ based sensor can be used as a convenient and simple method tool for anti-cancer treatment guidance and monitoring to sensitively detect the trace concentrations of PGE₂ and 8-HOA. Instead of using heavy, expensive and time-consuming GC-MS to assist the anti-cancer treatment, Ti₃C₂ based sensor can provide a faster, easier, efficient and much less invasive assistant tool to detect and cure cancer.

References

1. Cancer. Available online: <https://www.who.int/news-room/fact-sheets/detail/cancer> (accessed on).
2. Small Cell Lung Cancer—Cancer Therapy Advisor. Available online: <https://www.cancertherapyadvisor.com/home/decision-support-in-medicine/imaging/small-cell-lung-cancer/> (accessed on).
3. Molina, J.R.; Yang, P.; Cassivi, S.D.; Schild, S.E.; Adjei, A.A. Non-small cell lung cancer: Epidemiology, risk factors, treatment, and survivorship. In *Proceedings of the Mayo Clinic Proceedings*; Elsevier Ltd.: Amsterdam, The Netherlands, 2008; Volume 83, pp. 584–594.
4. Torre, L.A.; Siegel, R.L.; Jemal, A. Lung cancer statistics. *Adv. Exp. Med. Biol.* **2016**, *893*, 1–19.
5. Asbestos Lung Cancer: Causes, Diagnosis & Treatment. Available online: <https://www.asbestos.com/cancer/lung-cancer/> (accessed on).
6. Deadliest Cancers Receive the Least Attention. Available online: <https://www.asbestos.com/featured-stories/cancers-that-kill-us/> (accessed on).
7. Dela Cruz, C.S.; Tanoue, L.T.; Matthay, R.A. Lung Cancer: Epidemiology, Etiology, and Prevention. *CME* **2011**, *32*, 605–644.
8. Lee, S.H. Chemotherapy for lung cancer in the era of personalized medicine. *Tuberc. Respir. Dis. (Seoul)* **2019**, *82*, 179–189.
9. Cheng, M.; Jolly, S.; Quarshie, W.O.; Kapadia, N.; Vigneau, F.D.; Kong, F.M. Modern radiation further improves survival in non-small cell lung cancer: An analysis of 288,670 patients. *J. Cancer* **2019**, *10*, 168–177.
10. Sandler, A.B.; Dubinett, S.M. COX-2 inhibition and lung cancer. *Semin. Oncol.* **2004**, *31*, 45–52.
11. Vega, O.M.; Abkenari, S.; Tong, Z.; Tedman, A.; Huerta-Yepez, S. Omega-3 Polyunsaturated Fatty Acids and Lung Cancer: Nutrition or Pharmacology? *Nutr. Cancer* **2020**, 1–21, doi:10.1080/01635581.2020.1761408.

12. Yin, Y.; Sui, C.; Meng, F.; Ma, P.; Jiang, Y. The omega-3 polyunsaturated fatty acid docosahexaenoic acid inhibits proliferation and progression of non-small cell lung cancer cells through the reactive oxygen species-mediated inactivation of the PI3K /Akt pathway. *Lipids Health Dis.* **2017**, *16*, 1–9.
13. Kouremenos, K.A.; Johansson, M.; Marriott, P.J. Advances in gas chromatographic methods for the identification of biomarkers in cancer. *J. Cancer* **2012**, *3*, 404–420.
14. Cancer-Diagnosis and Treatment-Mayo Clinic. Available online: <https://www.mayoclinic.org/diseases-conditions/cancer/diagnosis-treatment/drc-20370594> (accessed on).
15. Problems with MRI for Cancer Diagnosis. Available online: <https://www.ctoam.com/precision-oncology/why-we-exist/standard-treatment/diagnostics/mri/> (accessed on).
16. The Pros and Cons of PET/CT Scans|Independent Imaging. Available online: <https://www.independentimaging.com/the-pros-and-cons-of-pet-ct-scans/> (accessed on).
17. Fred, H.L. Drawbacks and limitations of computed tomography: Views from a medical educator. *Texas Hear. Inst. J.* **2004**, *31*, 345–348.
18. Bitencourt, A.G.V.; Graziano, L.; Guatelli, C.S.; Albuquerque, M.L.L.; Marques, E.F. Ultrasound-guided biopsy of breast calcifications using a new image processing technique: Initial experience. *Radiol. Bras.* **2018**, *51*, 106–108.
19. Endoscopy: Purpose, Procedure, Risks. Available online: <https://www.webmd.com/digestive-disorders/digestive-diseases-endoscopy#1> (accessed on).
20. Gas Chromatography. Available online: http://www.chemforlife.org/teacher/topics/gas_chromatography.htm (accessed on).
21. Buszewski, B.; Ligor, T.; Jezierski, T.; Wenda-Piesik, A.; Walczak, M.; Rudnicka, J. Identification of volatile lung cancer markers by gas chromatography-mass spectrometry: Comparison with discrimination by canines. *Anal. Bioanal. Chem.* **2012**, *404*, 141–146.
22. Borer, J.S.; Simon, L.S. Cardiovascular and gastrointestinal effects of COX-2 inhibitors and NSAIDs: Achieving a balance. *Arthritis Res. Ther.* **2005**, *7*, S14.
23. Yang, P.; Chan, D.; Felix, E.; Cartwright, C.; Menter, D.G.; Madden, T.; Klein, R.D.; Fischer, S.M.; Newman, R.A. Formation and antiproliferative effect of prostaglandin E3 from eicosapentaenoic acid in human lung cancer cells. *J. Lipid Res.* **2004**, *45*, 1030–1039.
24. Xu, Y.; Qi, J.; Yang, X.; Wu, E.; Qian, S.Y. Free radical derivatives formed from cyclooxygenase-catalyzed dihomo- γ -linolenic acid peroxidation can attenuate colon cancer cell growth and enhance 5-fluorouracil's cytotoxicity. *Redox Biol.* **2014**, *2*, 610–618.
25. Xu, Y.; Yang, X.; Wang, T.; Yang, L.; He, Y.Y.; Miskimins, K.; Qian, S.Y. Knockdown delta-5-desaturase in breast cancer cells that overexpress COX-2 results in inhibition of growth, migration and invasion via a dihomo- γ -linolenic acid peroxidation dependent mechanism. *BMC Cancer* **2018**, *18*, 1–15.
26. Pang, L.; Shah, H.; Wang, H.; Shu, D.; Qian, S.Y.; Sathish, V. EpCAM-Targeted 3WJ RNA Nanoparticle Harboring Delta-5-Desaturase siRNA Inhibited Lung Tumor Formation via DGLA Peroxidation. *Mol. Ther. -Nucleic Acids* **2020**, *22*, 222–235.
27. Yang, X.; Xu, Y.; Wang, T.; Shu, D.; Guo, P.; Miskimins, K.; Qian, S.Y. Inhibition of cancer migration and invasion by knocking down delta-5-desaturase in COX-2 overexpressed cancer cells. *Redox Biol.* **2017**, *11*, 653–662.
28. Jafarizadeh-Malmiri, H.; Sayyar, Z.; Anarjan, N.; Berenjian, A.; Jafarizadeh-Malmiri, H.; Sayyar, Z.; Anarjan, N.; Berenjian, A. Nano-sensors in Food Nanobiotechnology. In *Nanobiotechnology in Food: Concepts, Applications and Perspectives*; Springer International Publishing: Berlin/Heidelberg, Germany, 2019; pp. 81–94.
29. Wang, P.; Zhang, L.; Zheng, W.; Cong, L.; Guo, Z.; Xie, Y.; Wang, L.; Tang, R.; Feng, Q.; Hamada, Y.; et al. Thermo-triggered Release of CRISPR-Cas9 System by Lipid-Encapsulated Gold Nanoparticles for Tumor Therapy. *Angew. Chem. -Int. Ed.* **2018**, *57*, 1491–1496.
30. Lei, Y.; Tang, L.; Xie, Y.; Xianyu, Y.; Zhang, L.; Wang, P.; Hamada, Y.; Jiang, K.; Zheng, W.; Jiang, X. Gold nanoclusters-assisted delivery of NGF siRNA for effective treatment of pancreatic cancer. *Nat. Commun.* **2017**, *8*, 1–15.
31. Li, N.; Wu, D.; Li, X.; Zhou, X.; Fan, G.; Li, G.; Wu, Y. Effective enrichment and detection of plant growth regulators in fruits and vegetables using a novel magnetic covalent organic framework material as the adsorbents. *Food Chem.* **2020**, *306*, 125455.

32. Wang, D.; Zhang, Q.; Hossain, M.R.; Johnson, M. High Sensitive Breath Sensor Based on Nanostructured K2W7O22 for Detection of Type 1 Diabetes. *IEEE Sens. J.* **2018**, *18*, 4399–4404.
33. Huber, F.; Riegert, S.; Madel, M.; Thonke, K. H2S sensing in the ppb regime with zinc oxide nanowires. *Sens. Actuators B Chem.* **2017**, *239*, 358–363.
34. Wang, C.; Chu, X.; Wu, M. Detection of H2S down to ppb levels at room temperature using sensors based on ZnO nanorods. *Sens. Actuators B Chem.* **2006**, *113*, 320–323.
35. Rai, P.; Majhi, S.M.; Yu, Y.T.; Lee, J.H. Noble metal@metal oxide semiconductor core@shell nano-architectures as a new platform for gas sensor applications. *RSC Adv.* **2015**, *5*, 76229–76248.
36. Korotcenkov, G.; Brinzari, V.; Cho, B.K. Conductometric gas sensors based on metal oxides modified with gold nanoparticles: A review. *Microchim. Acta* **2016**, *183*, 1033–1054.
37. Wang, D.L.; Chen, A.T.; Zhang, Q.F.; Cao, G.Z. Room-Temperature Chemiresistive Effect of TiO₂ Nanowires to Nitroaromatic and Nitroamine Explosives. *IEEE Sens. J.* **2011**, *11*, 1352–1358.
38. Wang, D.; Sun, H.; Chen, A.; Jang, S.H.; Jen, A.K.Y.; Szep, A. Chemiresistive response of silicon nanowires to trace vapor of nitro explosives. *Nanoscale* **2012**, *4*, 2628–2632.
39. Wang, T.; Huang, D.; Yang, Z.; Xu, S.; He, G.; Li, X.; Hu, N.; Yin, G.; He, D.; Zhang, L. A Review on Graphene-Based Gas/Vapor Sensors with Unique Properties and Potential Applications. *Nano-Micro Lett.* **2016**, *8*, 95–119.
40. Toda, K.; Furue, R.; Hayami, S. Recent progress in applications of graphene oxide for gas sensing: A review. *Anal. Chim. Acta* **2015**, *878*, 43–53.
41. Ji, J.; Wen, J.; Shen, Y.; Lv, Y.; Chen, Y.; Liu, S.; Ma, H.; Zhang, Y. Simultaneous Noncovalent Modification and Exfoliation of 2D Carbon Nitride for Enhanced Electrochemiluminescent Biosensing. *J. Am. Chem. Soc.* **2017**, *139*, 11698–11701.
42. Tan, C.; Cao, X.; Wu, X.J.; He, Q.; Yang, J.; Zhang, X.; Chen, J.; Zhao, W.; Han, S.; Nam, G.H.; et al. Recent Advances in Ultrathin Two-Dimensional Nanomaterials. *Chem. Rev.* **2017**, *117*, 6225–6331.
43. Wen, W.; Song, Y.; Yan, X.; Zhu, C.; Du, D.; Wang, S.; Asiri, A.M.; Lin, Y. Recent advances in emerging 2D nanomaterials for biosensing and bioimaging applications. *Mater. Today* **2018**, *21*, 164–177.
44. Ghidui, M.; Lukatskaya, M.R.; Zhao, M.Q.; Gogotsi, Y.; Barsoum, M.W. Conductive two-dimensional titanium carbide “clay” with high volumetric capacitance. *Nature* **2015**, *516*, 78–81.
45. Peng, Q.; Guo, J.; Zhang, Q.; Xiang, J.; Liu, B.; Zhou, A.; Liu, R.; Tian, Y. Unique lead adsorption behavior of activated hydroxyl group in two-dimensional titanium carbide. *J. Am. Chem. Soc.* **2014**, *136*, 4113–4116.
46. Michael, J.; Qifeng, Z.; Danling, W. Titanium carbide MXene: Synthesis, electrical and optical properties and their applications in sensors and energy storage devices. *Nanomater. Nanotechnol.* **2019**, *9*, 184798041882447.
47. Alhabeab, M.; Maleski, K.; Anasori, B.; Lelyukh, P.; Clark, L.; Sin, S.; Gogotsi, Y. Guidelines for Synthesis and Processing of Two-Dimensional Titanium Carbide (Ti₃C₂T_x MXene). *Chem. Mater.* **2017**, *29*, 7633–7644.
48. Pang, L.Z.; Shah, H.; Zhao, P.J.; Qian, S. New Delta-5-Desaturase Inhibitor Suppress Lung Cancer Progression: A Paradigm Shift on COX-2 Biology in Lung Cancer Treatment. *Fasbeeb J.* **2020**, *32*, 1.

Publisher’s Note: MDPI stays neutral with regard to jurisdictional claims in published maps and institutional affiliations.



© 2020 by the authors. Submitted for possible open access publication under the terms and conditions of the Creative Commons Attribution (CC BY) license (<http://creativecommons.org/licenses/by/4.0/>).